# Time-of-flight of solitary waves in dry and wet chains of beads: experimental results

R. Labbé
*Laboratorio de Turbulencia, Departamento de Física, Facultad de Ciencia, Universidad de Santiago de Chile, USACH. Casilla 307, Correo 2, Santiago, Chile*

I. Olivares and L. Vergara
*Departamento de Física, Facultad de Ciencia, Universidad de Santiago de Chile, USACH. Casilla 307, Correo 2, Santiago, Chile*

(Dated: January 26, 2017)

The speed of a solitary wave in a chain of beads is a function of its amplitude, and the details of the beads' contact force. By varying the amplitude of the incoming pulse, and measuring the time-of-flight (ToF), the effect that an added fluid has on the contact force was investigated. It was found that the fluid's rheological properties have non trivial effects on the ToF. This suggests that the ToF of the solitary wave could be a good measurable magnitude characterizing some of the rheological properties of the fluid surrounding the beads' contact points.

arXiv:1701.07133v1 [physics.flu-dyn] 25 Jan 2017

The mechanical properties of the contact between solid spheres are of considerable interest in applications involving high stresses on solid surfaces. An extensively used approach to tackle this problem consists in studying the propagation of solitary waves through chains of beads made of the material of interest [1–4]. The interaction of one of the ends of the chain with an external medium has been proven useful as a diagnostic tool of anomalies in that medium [5, 6]. Given that the time-of-flight (ToF)—the travel time of a pulse through the whole chain—depends on the individual interactions taking place between the beads during the pulse propagation, we expect a clear dependence of this global magnitude on the properties of those interactions. Measurements of wave propagation and ToF in 1D chains and 2D lattices under different conditions of the contact force were reported by Coste and Gilles [7, 8]. In addition, measurements of the ToF in dry and wet chains have been performed previously by Nesterenko *et al.* [9] and Job *et al.* [10]. In this work, we have made a detailed study of the effect that the amplitude of the incoming pulse has on the ToF in a dry chain, and the changes produced when the interaction force between the beads is slightly modified by a small volume of oil deposited on, and around the beads' points of contact. To this end, an automated device, capable of controlling the amplitude of the wave with nearly arbitrary resolution, was developed. Our results show that the speed of the solitary wave displays a much richer behavior than merely the increase found in previous works. In addition, these results suggest that the methods used here might be useful to test theoretical models of the contact forces between beads, including the modifications introduced by the addition of foreign materials—fluids in the present case—on the contact points. In our specific case, a study of the propagation of pulses in a chain of stainless steel (type 360) beads of diameter 0.5 inch was made, aimed to unveil the effect of the presence of a small volume of oil on the points of contact between the spheres. To assess the effect of a change in the rheological properties of the fluid, three different types of oil were used.

In precise terms, the system of interest may be described as follows: $N$ identical beads of mass $m$ arranged in a row are in contact and at rest in their equilibrium positions. The displacement of the bead $i$, $i = 1, ..., N$, from its equilibrium position is quantified by the coordinate $\delta_i$, and its equation of motion is

$$m\ddot{\delta}_i = f(\Delta_{i-1}, \dot{\Delta}_{i-1}, ..., t) - f(\Delta_i, \dot{\Delta}_i, ..., t) + g_i(\delta_i), \quad (1)$$

where $f$ is the interaction force between the beads, $\Delta_i = \delta_{i+1} - \delta_i$, and $g_i$ represent the interaction of each bead with the environment, including a small, positive constant force applied to the bead at the site $i = 1$, and a small force in each site to ensure the contact between the beads. It can be assumed that the forces $g_i$ are nearly the same for all $i > 1$, and have a very small dependence on $\delta_i$. The bead $N$, in contact with a semi sphere attached to a fixed wall, is subject to the condition $\delta_{N+1} = 0$. There is a bead acting as the striker at the opposite end. Its position is denoted as $\delta_0$, and its initial conditions are $\delta_0(t = 0) = x_0 \leqslant 0$, and $v_s = v_0 > 0$. We are interested in studying experimentally the effect that changes in the function $f$ have on the ToF of the solitary waves. For our purposes, we do not need a complete knowledge of $f$. We only assume that, at worst, its dependence on time is very weak. Considering that the ToF is a functional of $f$, our procedure will consist in comparing the ToF of solitary waves traveling on wet chains with the ToF obtained on a dry chain, for a number of values of $v_0$. This will allow making a quantitative assessment of the changes in the ToF due to different types of fluids between the beads or, equivalently, different variations of $f$.

In several aspects our experimental setup is similar to those used in the already mentioned works. Its main components are displayed in Figure 1. A track made of three parallel rods of silver steel, with diameter 5 mm and a separation of 6.05 mm between the axes of the lower pair, aligns the beads in a row. The upper rod does not touch the balls, and serves merely to secure accessories. The track assembly is attached to a brass bar with mass

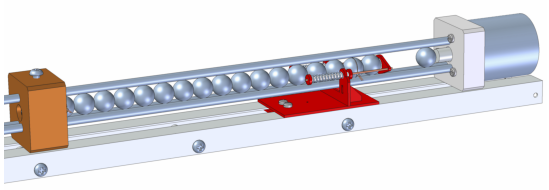


FIG. 1. Drawing of the main components of the bead chain collider. To the right, the electromagnetic actuator is shown, ready to fire the striker. The brass block on the left holds the stop, with a piezoelectric sensing element bonded to the latter. In this drawing, the second ball in the row also has a piezoelectric sensor. Near the center, the device in red exerts a compression force on the chain by means of two soft springs (see text).

$\sim 6$ kg (not pictured). At the left end, a brass block can be seen. A 12.7 mm diameter cylindrical stop made of steel is firmly tied to its center. This block is fastened to two brass rods (not displayed) making a total mass of $\sim 4.5$ kg. It can be displaced to accommodate chains of variable length, up to about 52 cm, allowing chains of up to 40 beads of diameter 0.5 inches. A circular piezoelectric ceramic disc is fixed to the flat face of the stop, and a half of a bead is fixed to the ceramic disk. This half sphere ends the chain. The arriving mechanical pulses are detected through the charge pumped by the ceramic disc in response to the compression force. The charge is converted into a voltage signal by a charge amplifier. A bead used as the striker impacts the right end of the chain, and produces a solitary wave. Its impulse is provided by an electromagnetic actuator —displayed at the right side of Figure 1— driven by a transconductance amplifier. The control signal is a bipolar pulse, calculated by a computer program, which sends it to the input of the transconductance amplifier through a 16 bit DAC interface. This signal is shaped using numerical results of the equations of motion of the actuator-striker system. Within a time interval of 5 ms, the actuator first accelerates the armature-striker mass, and then decelerates the armature. Finally, by applying a small current the armature is gently pulled back to its idle position, leaving the system armed for a new shot. To avoid gaps between the beads, a device with two soft springs gently pushes the first bead against the chain with an adjustable force $F \approx 0.24$ N. In addition, the track has a slight inclination of less than one degree, to obtain an idle contact force between the beads as small and uniform as possible. Our experimental setup can generate solitary waves through the chain of beads using striker speeds from some 0.05 m/s through about 2.5 m/s, with a theoretical resolution of about $1.5 \times 10^{-4}$ m/s. To measure the travel time of the wave, a bead with a piezoelectric ceramic is inserted at the site $i = 7$. The time between the maxima of the pulses on this site and the ceramic at the end of the chain defines the ToF through the beads in-between. As only the ToF is of interest here, and given that the signals from both transducers do not overlap in time, they were added into a single channel to maximize the time resolution of the acquired data. Once programmed, this completely automated setup works autonomously, which allows acquiring the large amount of data required for statistical purposes. An auxiliary device, also controlled by the computer program and not shown in Figure 1, places the striker in contact with the actuator pusher before each shoot. Also omitted in Figure 1 is a photogate designed for precise measurement of the striker speed just before its impact with the chain. This proved necessary in view of several sources of uncertainty present in the shooting device. All of the data generated after each shoot was acquired by the same program, through a 16 bit ADC interface working at 500 kS/s per channel, or one channel at 1.0 MS/s, when a better time resolution was needed. The four cases reported here (the dry chain, and wet chains using three types of oil) required a running time of about 12 hours each, and a total of $4.8 \times 10^8$ data points. A description in full detail of the experimental device will be published elsewhere.

The experimental results shown here were obtained using striker speeds from $0.075 \pm 0.003$ m/s through $1.23 \pm 0.003$ m/s, where the uncertainty was calculated as the standard deviation over 20 shots. At moderately high speeds, it was observed that at equal impact speeds the rebound speeds of the striker were noticeably different. Subsequently, small motions of the beads along the chain were detected. This suggested that tiny gaps between the beads were generated after the passage of the solitary wave. We performed some numerical simulations, which confirmed that observation. In fact, several authors have studied the fragmentation, and the effects of dispersion, on a line of balls [11–13]. Thus, a change in the methodology was in order. At speeds below $\sim 0.25$ m/s, no rebound of the striker was observed. Then, before each measurement the striker was used to give a series of taps to the chain, using a speed $v_t = 0.18$ m/s. In principle, this should compactify the chain. To make sure that no gaps remained in the chain, prior to each measurement 40 taps at $v = v_t$ were given. Of course, this made the time necessary for an experiment 40 times longer than an experiment without tapping. It must be remarked that a tapping technique was previously used by several other authors to increase the packing density of granular materials [14, 15]. Summarizing, each point in the following figures was obtained by repeating 20 times the sequence of giving 40 taps, and then shooting the striker at the desired speed to measure the ToF.

In Figure 2, four curves represent the signals generated by the piezoceramic transducers. The pulses at their centers, whose maxima have been associated to the instant $t = 0$, correspond to the arrival of the solitary wave to the fixed wall. The pulses on the left, with $t < 0$, represent the wave passing through the site $i = 7$, while the pulses

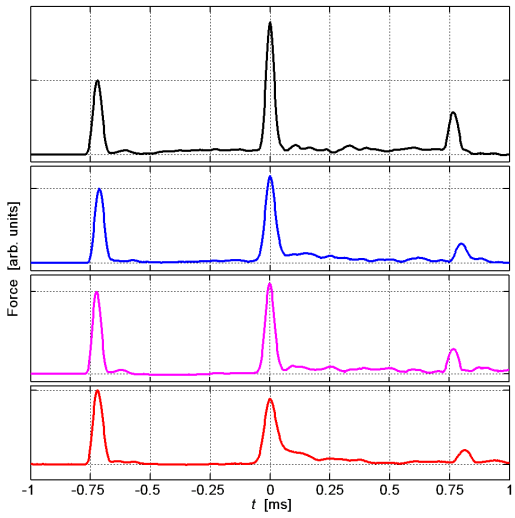



FIG. 2. Signals from the piezoceramic sensors when the impactor speed is $v_s \approx 0.82$ m/s, normalized to the maximum of the incoming pulse. In all of the plots, $t = 0$ is fixed to the maximum of the pulse in the wall. The pulses for $t < 0$ correspond to the incoming wave passing through the ball at the site $n = 7$, while the pulses for $t > 0$ correspond to the reflected wave passing through the same site. The top curve corresponds to the dry chain. The remaining curves from top to bottom were obtained with different types of oil between the beads: DS19 vacuum pump oil, SAE 0W-30 synthetic motor oil, and EP 80W-90 gear oil, respectively. It can be seen that the presence of the fluid increases the attenuation of the wave, and modifies the time of flight to a certain extent (see text).

on the right, with $t > 0$, represent the reflected wave passing through the same site. All the pulses in these plots were produced using the same speed for the striker: $v_s \approx 0.82$ m/s. If there were conservation of momentum, the area under the pulses at the center should be twice the area under the pulses at the left side, because of the momentum reversal. However, the momentum is not conserved in this system due to the interaction of the beads with the track. In addition, when the amplitude of the wave surpasses a given threshold, at each contact point there is a small rebound, leading to the chain fragmentation mentioned earlier. These two effects explain the size of the central peaks. There is also a small momentum transfer to the wall, but in view of the mass ratio between a bead and the wall, this last transfer should not be greater than 0.2%. In the same Figure, it can be clearly seen that the ToF of the reflected wave is greater in all cases. This is due in part to its smaller amplitude and in part to the chain loosening by the propagation of the pulse before its reflection. Nevertheless, it can be noticed that all of the pulses have nearly the same width, evidencing the non-dispersive character of the propagation.

In Figure 3 a plot of the ToF on the dry chain is displayed. The lower data correspond to the solitary wave traveling towards the fixed wall, while the upper data represent the ToF of the reflected wave. As expected, the ToF is larger in the latter case. It is also clear that the uncertainty of the data is greater for the reflected wave. These two effects are explained as follows: when the wave is traveling towards the wall, the propagation takes place on a chain compacted by the tapping process. But the wave leaves behind a loosened chain, which is the medium where the reflected wave propagates. This increases both, the ToF and its uncertainty. Without loosening, the increase in the ToF of the reflected pulse would be smaller. The lower data shows clearly the dependence of the ToF on the speed of the striker. Of course, the amplitude of the solitary wave is expected to be a strictly increasing function of the striker's speed, which is confirmed by the experimental data: higher impactor speeds lead to larger wave amplitudes, which in turn lead to faster propagation speeds and smaller ToFs. In what follows, the lower data are used as the reference for comparison with the data obtained on wet chains.

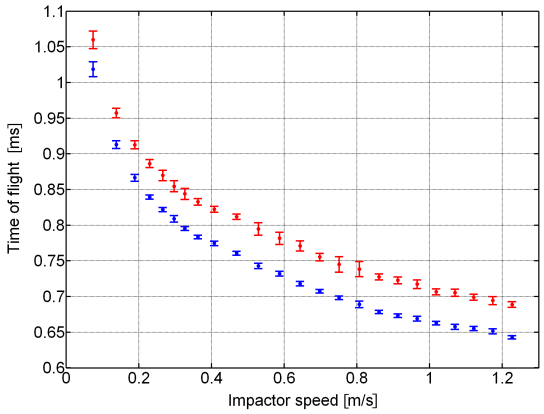



FIG. 3. ToF in a dry chain made of stainless steel beads, as a function of the impactor speed. The lower points correspond to the ToF of waves traveling towards the fixed wall, while the upper points are the ToF of the reflected waves. Note that both, the ToF and uncertainties are larger for the upper data. (see text).

Figure 4 displays the effect of adding a drop of oil on the contact points of the beads between the sensor at site $i = 7$ and the wall. Three types of oil were used: triangles correspond to DS19 rotary vacuum pump oil; squares were obtained using SAE 0W-30 synthetic motor oil; and filled circles correspond to EP 80W-90 gear oil. The exact rheological properties of these fluids are unknown. For the DS19 oil, it is known that it consists essentially of hydrocarbons. The curve of kinematic viscosity as a function of temperature is provided by the manufacturer, so, at the working temperature $\theta = 23°$C, the kinematic viscosity is $\nu \approx 130$ cSt. As can be seen, the ratio $T_{\rm wet}/T_{\rm dry}$ for the DS19 oil is less than one for impactor speeds below 1.1 m/s, meaning that the ToF

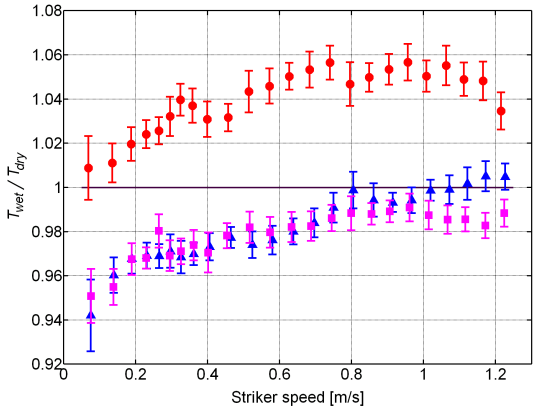



FIG. 4. Ratios of ToF in wet chains to that in a dry chain. Triangles correspond to rotary vacuum pump oil, squares correspond to synthetic motor oil, and filled circles correspond to gear oil (see text).

is smaller than that on the dry chain or, equivalently, that the propagation speed of the solitary wave is larger. For impactor speeds greater than 1.1 m/s we see the opposite. Although there are some regions where the ToF decreases while the impactor speed increases, the trend of the data is mainly increasing. The data represented in squares follow a similar trend, except that at higher impactor speeds the ratio $T_{\rm wet}/T_{\rm dry}$ remains below one. In this case, the propagation speed is always larger than that in the dry chain. Interestingly, the behavior with gear oil is very different. As the filled circles show, the ToF is greater than that in the dry chain, meaning that the propagation speed in this case is always smaller, but the general trend somewhat resembles the behavior of the motor oil. Thus, as mentioned earlier, our results reveal a complex behavior, not seen in previous works. At present we do not have a quantitative model for these findings, but a qualitative analysis can be attempted. It is clear that at faster impactor speeds the rate of strain on the contact points is larger. So, the oil around those points must flow faster. As the viscosity limits the flow rate, the ToF should be roughly a decreasing function of the impactor speed. Due to the geometry of the surfaces confining the fluid, and the way they evolve during the passage of the wave, the inertia of the fluid should contribute similarly to this trend. This is seen when the impactor speeds are above 0.95 m/s, but for the motor and gear oils only. Below this speed, in all of the cases we see roughly the opposite behavior. Summarizing, for increasing amplitudes of the wave, the hydrocarbon based oil gives an essentially increasing trend of the ToF, passing from values smaller than that that in the dry chain, to values slightly larger. The motor and gear oils have a global maximum, and their ToF remain below or above of that of the dry chain, respectively. For a detailed explanation of these behaviors, especially the increasing trend of the three cases when the impactor speed is below 0.95 m/s, a theoretical model incorporating a detailed knowledge of the rheological properties of the fluids is required, beyond previous efforts to elucidate the effects of viscosity and inertia in the flow between flat surfaces [16, 17]. Probably the behaviors of the motor and gear oils, as compared to DS19 oil, are related to some non Newtonian characteristic conferred by additives used in these oils to improve their performance. This suggests that measurements of ToF in bead chains under appropriate conditions could make them useful as instruments to measure the rheological properties of fluids.

The authors gratefully acknowledge C. Daraio and P. Anzel for sharing their experience on the use of piezoceramic transducers. Financial support for this work was provided by FONDECYT grants No. 1130492, and No. 1040291.

[1] V. Nesterenko, J. Appl. Mech. and Tech. Phys. **24**, 733 (1983).
[2] A. Lazaridi and V. Nesterenko, J. Appl. Mech. and Tech. Phys. **26**, 405 (1985).
[3] C. Coste, E. Falcon, and S. Fauve, Phys. Rev. E **56**, 6104 (1997).
[4] C. Daraio, V. Nesterenko, E. Herbold, and S. Jin, Phys. Rev. E **72**, 016603 (2005).
[5] D. Khatri, C. Daraio, and P. Rizzo, in *The 15th International Symposium on: Smart Structures and Materials & Nondestructive Evaluation and Health Monitoring* (International Society for Optics and Photonics, 2008) pp. 69340U–69340U.
[6] J. Yang, C. Silvestro, D. Khatri, L. De Nardo, and C. Daraio, Phys. Rev. E **83**, 046606 (2011).
[7] C. Coste and B. Gilles, EPJB **7**, 155 (1999).
[8] B. Gilles and C. Coste, Phys. Rev. Lett. **90**, 174302 (2003).
[9] E. B. Herbold, V. F. Nesterenko, and C. Daraio, in *Shock Ccompression of Condensed Matter-2005: Proceedings of the Conference of the American Physical Society Topical Group on Shock Compression of Condensed Matter*, Vol. 845 (AIP Publishing, 2006) pp. 1523–1526.
[10] S. Job, F. Santibanez, F. Tapia, and F. Melo, Ultrasonics **48**, 506 (2008).
[11] F. Herrmann and P. Schmälzle, Am. J. Phys. **49**, 761 (1981).
[12] F. Herrmann and M. Seitz, Am. J. Phys. **50**, 977 (1982).
[13] E. J. Hinch and S. Saint-Jean, Proc. R. Soc. Lond. A **455**, 3201 (1999).
[14] J. B. Knight, C. G. Fandrich, C. N. Lau, H. M. Jaeger, and S. R. Nagel, Phys. Rev. E **51**, 3957 (1995).
[15] P. Philippe and D. Bideau, Europhys. Lett. **60**, 677 (2002).
[16] S. Weinbaum, C. Lawrence, and Y. Kuang, J. Fluid Mech. **156**, 463 (1985).
[17] C. Lawrence, Y. Kuang, and S. Weinbaum, J. Fluid Mech. **156**, 479 (1985).